Developmental Biology 353 (2011) 382–395

Contents lists available at ScienceDirect

Developmental Biology

journal homepage: www.elsevier.com/developmentalbiology

Genomes & Developmental Control

Genomically integrated transgenes are stably and conditionally expressed in neural crest cell-specific lineages

Yasuhiro Yokota [a], Daisuke Saito [a,b], Ryosuke Tadokoro [a,b], Yoshiko Takahashi [a,b,*]

[a] Graduate School of Biological Sciences, Nara Institute of Science and Technology, 8916–5, Takayama, Ikoma, Nara, 630–0192, Japan
[b] JST, CREST, Japan

ARTICLE INFO

Article history:
Received for publication 14 October 2010
Revised 8 January 2011
Accepted 1 February 2011
Available online 17 February 2011

Keywords:
Neural crest
Enhancer, Tol2-transposon
Electroporation
Tet-on inducible expression
Cre-loxP
Transgenesis
Sensory neurons
Schwann cells
Melanocytes

ABSTRACT

Neural crest cells (NCCs) are a transient embryonic structure that gives rise to a variety of cells including peripheral nervous system, melanocytes, and Schwann cells. To understand the molecular mechanisms underlying NCC development, a gene manipulation of NCCs by in ovo electroporation technique is a powerful tool, particularly in chicken embryos, the model animal that has long been used for the NCC research. However, since expression of introduced genes by the conventional electroporation method is transient, the mechanisms of late development of NCCs remain unexplored. We here report novel methods by which late-developing NCCs are successfully manipulated with electroporated genes. Introduced genes can be stably and/or conditionally expressed in a NCC-specific manner by combining 4 different techniques: Tol2 transposon-mediated genomic integration (Sato et al., 2007), a NCC-specific enhancer of the *Sox10* gene (identified in this study), Cre/loxP system, and tet-on inducible expression (Watanabe et al., 2007). This is the first demonstration that late-developing NCCs in chickens are gene-manipulated specifically and conditionally. These methods have further allowed us to obtain ex vivo live-images of individual Schwann cells that are associated in axon bundles in peripheral tissues. Cellular activity and morphology dynamically change as development proceeds. This study has opened a new way to understand at the molecular and cellular levels how late NCCs develop in association with other tissues during embryogenesis.

Introduction

During vertebrate development, the neural crest (NC) is a transient structure that gives rise to a variety of tissues, including all types of peripheral nervous system in the trunk. Neural crest cells (NCCs) emigrate from the dorsal aspect of the neural tube, and migrate over distances in the body to their destinations, where they undergo terminal differentiation (Le Douarin and Kalcheim, 1999). An increasing body of knowledge accumulates regarding the molecular mechanisms by which neural crest specification and early emigration are regulated (Knecht and Bronner-Fraser, 2002; Meulemans and Bronner-Fraser, 2004). For these studies, a gene manipulation technique serves as a powerful tool. In particular, in chicken embryos that have long been used as a most suitable model animal for the NC study, the in ovo electroporation technique (Funahashi et al., 1999; Momose et al., 1999) has enabled NCC transgenesis (Harris et al., 2008; McKeown et al., 2005; Petiot et al., 2002; Tucker, 2001). In most cases for the NC-transgenesis, exogenous genes are introduced into an early neural tube, from which NCCs emigrate carrying these genes.

However, the usefulness of the electroporation technique has been limited to earlier events of NCCs: since electroporated genes are not integrated into the genome, their copies become diluted and ultimately disappear as NCCs undergo massive proliferation. Thus, the molecular mechanisms underlying later development of NCC-derived lineages remain largely unexplored. During late stages in the trunk, a variety of important events occur in NCC-derivatives: melanocytes, sensory neurons, Schwann cells and others undergo terminal differentiation and start exhibiting their characteristics of physiological functions. For instance, Schwann cells, the precursor of myelin sheaths, become intimately associated with axons in peripheral tissues.

Toward understanding the molecular mechanisms underlying the late development of NCCs, we have in this study developed novel gene manipulation methods that offer three major advantages; long-term expression, NCC-specific expression, and conditionally inducible expression. First, long-term expression is achieved by the Tol2-mediated genomic integration method, which we recently established (Sato et al., 2007). Second, NCC-specific expression is enabled by a NCC-specific enhancer of *Sox 10* gene, identified in this study. Further combination with Cre/loxP system (Gu et al., 1994; Hamilton and Abremski, 1984; Lobe et al., 1999; Nagy, 2000) allows NCC-specific and long-term expression of introduced EGFP. Third, the tetracycline-dependent expression system (tet-on; Watanabe, et al., 2007; Sato, et al., 2007) is applied to conditionally express exogenous genes at a desired time point

* Corresponding author at: Graduate School of Biological Sciences, Nara Institute of Science and Technology, 8916–5, Takayama, Ikoma, Nara, 630–0192, Japan. Fax: +81 743 72 5559.
E-mail address: yotayota@bs.naist.jp (Y. Takahashi).

0012-1606/$ – see front matter © 2011 Elsevier Inc. All rights reserved.
doi:10.1016/j.ydbio.2011.02.001

during late development of NCCs. These methods enable sensory neurons, Schwann cells, and melanocytes in peripheral tissues to be EGFP-labeled in a genetically manipulable manner. Furthermore, we have performed live-imaging microscopy to directly visualize EGFP-labeled Schwann cells using ex vivo cultured tissues. These cells actively extend and retract cellular processes prior to cellular elongation along peripheral axon bundles. Thus, this study has opened a new way to understand at the molecular and cellular levels how late NCCs develop in association with neighboring tissues during embryogenesis.

Materials and methods

Embryological manipulations

Commercially available chicken eggs were delivered from poultry farm, and basic techniques and electroporation were as previously described (Sato et al., 2002). A DNA solution was injected into the central canal of the neural tube of E2 embryo. Electric pulses of 12 V, 25 ms were charged five times with 975-ms intervals.

Genomic clones of chicken Sox10 locus

Genomic fragments in a 5′ UTR region of *Sox10* ORF were amplified with KOD-Plus-ver.2 (TOYOBO), using BAC DNA clones as the template (CH261-72C6, BACPAC Resources; Tam33-18P11, GENEfinder Genomic Resources, Texas A&M University). Each fragment, ranging from 0.6 kb to 10 kb in size, was cloned into either SalI, BglII, XhoI, or SmaI site of ptkEGFP vector. The ptkEGFP reporter vector (gift from Dr. Kondoh, Osaka University) possesses Herpes simplex virus thymidine kinase basic promoter (tk) upstream of EGFP (Uchikawa et al., 2003). Successful subcloning for each genomic fragment was verified by partial sequencing of the terminal region.

Vector constructions

pT2K-CAGGS-EGFP, pCAGGS-T2TP, and pT2K-BI-TRE-EGFP

These constructs were previously described in Sato et al., 2007.

pCAGGS-mCherry and pT2K-CAGGS-mCherry

mCherry cDNA (Clontech) was subcloned into the XhoI site of pCAGGS (Momose et al., 1999) to make pCAGGS-mCherry, from which mCherry was digested with EcoRI-EcoRV, and subcloned into the same sites of pT2K-CAGGS (Sato et al., 2007) to make pT2K-CAGGS-mCherry.

pT2K-enhancer$^{4\text{-}1}$-tkEGFP

pEnhancer$^{4\text{-}1}$-tkEGFP was digested with KpnI–SpeI to obtain the fragment containing enhancer$^{4\text{-}1}$ and tkEGFP, which was subsequently subcloned into ApaI–BglII site of pT2K-BI-TRE-EGFP after blunt ended.

pCAGGS-Cre

This is the same as pxCANCre, which was originally reported in Kanegae et al. (1996). In this study, we describe pxCANCre (pCAGGS-Cre).

pEnhancer$^{4\text{-}1}$-tk-Cre

pEnhancer$^{4\text{-}1}$-tk-Cre is a derivative of pEnhancer$^{4\text{-}1}$-tkEGFP. First, ptk-Cre was constructed: the cDNA fragment encoding nuclear localizing signal (NLS)-fused Cre (Kanegae et al., 1996) was subcloned into ptkEGFP at the site of StyI and NdeI, in between tk and SV40-ployA to replace EGFP. Subsequently, enhancer$^{4\text{-}1}$ (SalI-sited) was inserted into SalI-digested ptk-Cre.

pT2K-CAGGS-loxP-DsRed2-loxP-EGFP

pCALNL5 (Kanegae et al., 1996) was manufactured so that the DsRed2-polyA fragment was inserted in between loxP sites of the plasmid. Subsequently, SmaI-sited EGFP was added after the second loxP. From this construct, a fragment spanning from the first loxP to EGFP was PCR-amplified, and inserted into the EcoRV site positioned between CAGGS and polyA of pT2K-CAGGS, to make the final construct of pT2K-CAGGS-loxP-DsRed2-loxP-EGFP.

pT2K-CAGGS-loxP-DsRed2-loxP-rtTA2^{S}-M2

The procedure was as described above (pT2K-CAGGS-loxP-DsRed2-loxP-EGFP) with rtTA2^{S}-M2 in place of EGFP. rtTA2^{s}-M2 is a kind gift of Dr. Hillen (Urlinger et al., 2000; Watanabe et al., 2007).

Comparative genomic analyses

Highly conserved genomic sequences between different species were searched by VISTA (http://pipeline.lbl.gov/cgi-bin/gateway2) (Mayor et al., 2000). Conserved genomic sequences with no lower than 60% identity continuing over 100 bp were selected.

DNA transfection with DF1 cells

The basic protocol was as described in Sato et al., 2007. DF1, an avian cell line purchased from ATCC (Himly et al., 1998), was maintained in Dulbecco's Modified Eagle's Medium containing 10% fetal bovine serum. 5×10^5 DF1 cells were plated and subjected to DNA transfection on the following day using Lipofectamine 2000 (Invitrogen) with DNA plasmids, the total amount of which not exceeding 4 μg (500 ng of pT2K-CAGGS-loxP-DsRed2-loxP-EGFP, pT2K-CAGGS-loxP-DsRed2-loxP-rtTA2^{S}-M2, pT2K-BI-TRE-EGFP, and pCAGGS-T2TP, 0.1 ng to 50 ng of pxCANCre). EGFP and DsRed2 signals were detected using AxioPlanII microscope with Apotome system (Carl Zeiss), or LSM5 PASCAL confocal laser scanning microscope (Carl Zeiss).

Administration of a doxycycline (Dox) solution

For developing embryos, as previously described (Watanabe et al., 2007), 500 μl of Dox solution (0.3 mg/ml in HANKS: 140 mM NaCl, 5.4 mM KCl, 5.6 mM glucose, 0.34 mM Na_2HPO_4, 10 mM HEPES, 1 mM $MgCl_2$, 1 mM $CaCl_2$ pH 7.0) was injected in between the embryo and yolk. For cultured DF1 cells, the Dox solution was added to the culture medium at the concentration of 1 μg/ml was added.

Western blotting

DF1 cells were treated with 4× sodium dodecyl sulfate (SDS) sample buffer (200 mM Tris–HCl, (pH 6.8), 8% SDS, 400 mM dithiothreitol, 0.2% bromophenol blue, 40% glycerol). The eluates were subjected to SDS-PAGE followed by immunoblotting with mouse anti-GFP monoclonal antibody (Santa Cruz), and HRP-conjugated sheep anti-mouse IgG antibody (Amersham). Signals for EGFP protein were revealed with the ECL Advance Western Blotting Detection kit (Amersham). Densitometric analysis was performed using the luminous image analyzer LAS-3000 mini (Fuji Film).

Immunohistochemistry

Immunohistochemistry with frozen sections was performed essentially as previously described (Sato et al., 2002; Watanabe et al., 2007). Embryos were fixed in 4% paraformaldehyde (PFA) at 4 °C overnight and immersed in a graded series of sucrose solutions up to 30%, then embedded in Tissue-Tek (Sakura). 10 μm cryostat sections were treated with 2% skim milk/PBS for 1 h at room temperature (RT), and incubated overnight at 4 °C in 1:500 dilution of HNK-1 antibody (Bio-Rad). After washing three times in PBS, the specimens were reacted with Alexa 568 goat anti-mouse IgM (Molecular Probes) with 1:500 dilution for 1 h at RT. The reaction was terminated by washing three times in PBS, and the sections were sealed by Fluoromount (Diagnostic BioSystems).

For immunohistochemistry with a flat-mount specimen, a surface tissue, mostly containing epidermis, was peeled from a flank region of

electroporated embryos, and fixed in 4% PFA at 4 °C overnight. For the detection of sensory neurons and melanocytes, the tissue was treated with 2% skim milk/PBS for 1 h at RT, and incubated overnight at 4 °C in 1:300 dilution of anti-Tuj1 antibody (R&D Systems), or in 1:100 dilution of anti-MITF antibody (Invitrogen). After washing three times in PBS, the specimens were reacted with Alexa 568 goat anti-mouse IgG with 1:500 dilution for 1 h at RT. The reaction was terminated by washing three times in PBS, followed by mounting in a slide glass as a flat specimen. For the detection of Schwann cells, fixed surface tissues were treated in TNB (0.1 M Tris–HCl pH7.5, 0.15 M NaCl, 0.05% Tween 20, Blocking Reagent (Roche)) for 1 h at RT, and incubated overnight at 4 °C in 1:300 dilution of anti-P0 antibody (1E8, Developmental Studies Hybridoma Bank). After washing three times in TNT(0.1 M Tris–HCl pH7.5, 0.15 M NaCl, 0.05% Tween 20), the specimens were reacted with Alexa 568 goat anti-mouse IgG with 1:500 dilution for 1 h at RT. The reaction was terminated by washing three times in TNT. EGFP signals and immunofluorescence were obtained using AxioPlanII microscope with Apotome system (Carl Zeiss).

In situ hybridization with Sox10 probe in histological sections

Chicken *Sox 10* cDNA was obtained by RT-PCR using the following primers: 5′-AATTCTCGAGATGGCTGATGACCAAGATCT-3′ (forward), and 5′-AATTGATATCCTATGGTCTGGAGAGAGTCG-3′ (reverse). Preparation of a digoxigenin-labeled probe, and section in situ hybridization was as previously described (Sato et al., 2002).

Ex vivo culture of sliced specimens and live-imaging microscopy

Ex vivo slice culture was performed as previously reported (Ohata et al., 2009) with some modifications. The “basic medium” was prepared with DMEM/Ham's F12 (Wako), 25 mM sodium bicarbonate, 15 mM HEPES, 50 IU/ml penicillin, and 50 mg/ml streptomycin. For a sample mounting, 1% low-melting-point agarose (Invitrogen) in DMEM/Ham's F12 medium, containing 1 mM sodium pyruvate, 5 mM glutamine, and 5 mg/ml fungizone, was prepared. Transverse slices of embryos of ~400 μm thick were prepared in the basic medium at RT using a sharpened microsurgical blade (FEATHER). The slices were mounted in a small volume of 1% agarose medium prepared in a 35 mm glass-bottom dish (MATSUNAMI). 10 min after mounting, the dish was filled with the culture medium. The specimens were placed in an incubation chamber connected to a LSM5 Pascal confocal laser scanning microscope (Carl Zeiss). Images were obtained and processed with LSM Image Browser software (Carl Zeiss).

Results and discussion

Stable transgenesis of NCCs by Tol2-mediated gene transfer

To stably introduce exogenous genes into NCCs, we combined the in ovo electroporation technique with the Tol2-transposon-mediated gene transfer method, which we previously optimized for somitic manipulation in chicken embryos (Sato et al., 2007). As described in that report, three kinds of plasmids were used (Fig. 1A): pCAGGS-T2TP (a plasmid containing a constitutive promoter (CAGGS) that drives cDNA encoding the transposase (T2TP) required for genomic integration), pT2K-CAGGS-EGFP (pT2K-vector carries Tol2-sequences necessary for genomic integration), and pCAGGS-mCherry (the plasmid used for short term monitoring of electroporation efficiency). These three plasmids were co-electroporated into early neural tube/neural crest at embryonic day 2 (E2). At E3 when a neural crest population started emigrating, both EGFP and mCherry signals were successfully observed in an overlapping set of cells (Fig. 1B, n = 26). In contrast, at E7 (5-day post electroporation), whereas mCherry signal (non-integrated) was hardly detected in dorsal root ganglion (DRG) probably due to a massive cell division of NCCs, EGFP signals were retained in these cells (Fig. 1C, n = 11). This was also quantitatively confirmed: the ratio of $EGFP^+$ cells over $mCherry^+$ cells increased as development proceeded (1.1 ± 0.2 at E3 to 5.7 ± 2.0 at E7, Fig. 1D). Thus, the Tol2-mediated gene transfer technique enables NCCs to be stably manipulated with electroporated genes. In contrast to NCCs, a significant number of cells remained mCherry-positive in the spinal cord (Fig. 1C). This is probably because precociously differentiated neurons that no longer undergo cell proliferation could harbor genomically non-integrated plasmids.

NCCs are known to give rise to a variety of cell types including sensory neurons, Schwann cells, and melanocytes. Indeed, we observed EGFP signals in these lineages at E7 (n = 7, Fig. 1E–G). Each cell type was confirmed by immuno-cytochemistry with antibodies against Tuj1, P0, and MITF, respectively, in a flat-mounted surface tissue peeled from the flank region of E7 embryos (Fig. 1).

NCC-specific manipulation using Sox10 enhancer

The gene manipulation described in Fig. 1 also caused stable expression of EGFP in motor neurons located in the ventral region of the spinal cord (Fig. 1C), from which motor axons are extended into peripheral tissues. Since motor axons are ensheathed by Schwann cells and also often accompanied with sensory neurons, it would be useful if NCCs could specifically be manipulated separately from motor neurons. To achieve this, we attempted to identify a NCC-specific enhancer of the *Sox10* gene, a member of SRY-box family, known to be specifically expressed in early NCCs (Betters et al., 2010; Cheng et al., 2000; Southard-Smith et al., 1998). We confirmed the NCC-specific expression of *Sox10* mRNA by comparing with HNK-1 signals, another NCC marker, in neighboring sections (Fig. 2A).

To identify a *Sox10* enhancer(s), we performed *in silico* genomic comparison that finds highly conserved non-coding elements (CNE) between different species. Genomic sequences spanning ~43 kb including the chicken *Sox10* open reading frame (ORF) were compared with the human genome using VISTA application (http://pipeline.lbl.gov/cgi-bin/gateway2). Seven different CNEs showing >60% homology within 100 bp were selected, among which five (red peaks) and two (light blue peaks, UTRs) were in the 5′- and 3′ regions of the *Sox10* gene, respectively (Fig. 2B, Table 1). For subsequent analyses, 8 overlapping genomic regions (#1–#8, Fig. 2B), containing zero to two of these CNEs, were obtained using chicken BAC clones that included *Sox10* genomic sequences. These 8 fragments and their further dissected fragments were individually inserted into the EGFP reporter plasmid, ptkEGFP (Fig. 2C) (Uchikawa et al., 2003), carrying the thymidine kinase (tk) basal promoter and EGFP. Thus, this reporter would express EFGP only when receiving an appropriated enhancer.

ptkEGFP inserted with each of 20 different candidate enhancers was co-electroporated with pCAGGS-mCherry into the neural tube of E2 embryo (Fig. 2C), and EGFP signal was assessed in migrating NCCs of E2.5 embryo. Such analyses identified three types of CNEs in regard to EGFP expression. First one was the expression specific to NCCs (blue boxes, including #4-1). The second was the expression seen in both NCCs and neural tube (gray boxes including #1-4), and the third showed no expression (white boxes) (Fig. 2B, Table 2. Fig. 2D shows two representative specimens: whole-mount- and transverse views of embryos electroporated with ptkEGFP-#1-4 (EGFP in neural tube and NCCs, n = 10) and ptkEGFP-#4-1 (EGFP specifically in NCCs, n = 10). The specific expression by #4-1 was also confirmed quantitatively: a ratio of the number of $EGFP^+$ cells over $mCherry^+$ cells in the neural tube was 0.054 ± 0.037 for ptkEGFP-#4-1, whereas 0.77 ± 0.161 for ptkEGFP-#1-4 (Fig. 2E). Importantly, $EGFP^+$ cells found in ptkEGFP-#4-1-electroporated embryos overlapped with endogenous *Sox10* mRNA-positive cells (Fig. 2D, n = 10). Together, we conclude that the fragment #4-1 (3571 bp long, the position −10,762 bp to −7192 bp), which contains CNE #3, acts as a NCC-specific enhancer of *Sox10* at least in early migrating NCCs. We hereafter refer this region #4-1 to enhancer$^{4\text{-}1}$. Enhancer$^{4\text{-}1}$, thus identified in this study independently, is found to overlap with an

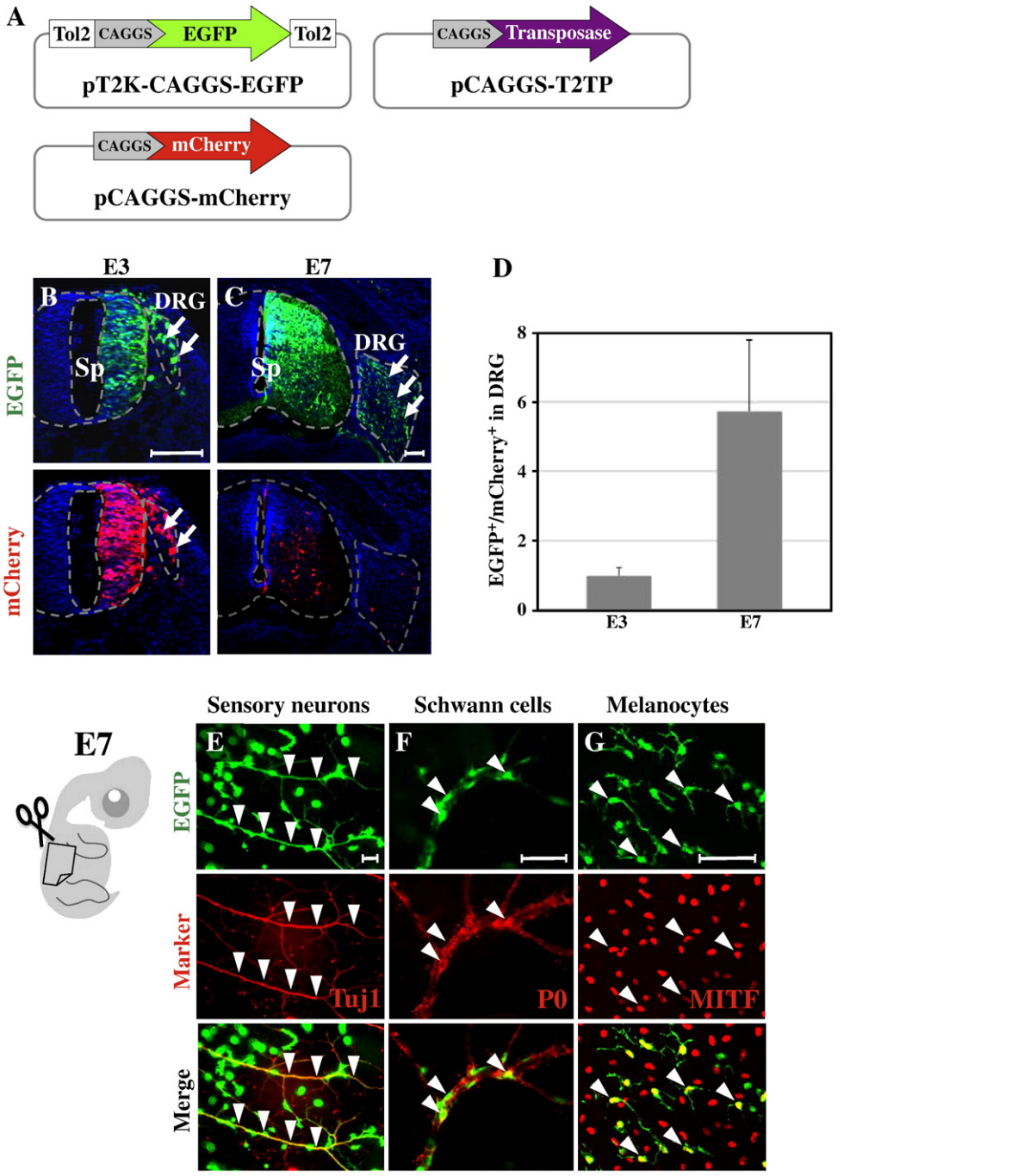

Fig. 1. Stable transgenesis of NCCs by Tol2-mediated gene transfer. (A) Three plasmids were co-electroporated into a neural tube of E2 embryo. (B, C) At E3, both EGFP- and mCherry signals were observed in the spinal cord (Sp) and developing DRG (arrows). By E7, although mCherry signal (not integrated) was extinguished, EGFP signal (integrated) was retained. Scale bar: 100 μm. (D) Retained expression of EGFP was quantitatively demonstrated by a ratio of the number of EGFP-positive cells over mCherry-positive cells in DRG. n = 12 for E3, n = 9 for E7. (E–G) EGFP signal was stably expressed in late-developing NCC-derived cells (arrowheads). A surface tissue including skin was peeled from the flank region of electroporated E7 embryo as shown in a diagram, and subjected to a preparation of flat-mount specimen. Sensory neurons, stained with Tuj1 (E), Schwann cells associated with peripheral axons, stained with P0 (F), and melanocytes in the skin, stained with MITF (G). Scale bar: 50 μm.

enhancer reported recently (Betancur et al., 2010), the activity of which was investigated mostly in the cephalic region.

Genomically integrated enhancer$^{4\text{-}1}$ recapitulates the endogenous expression of Sox10 mRNA in developing DRG

We further examined whether the enhancer$^{4\text{-}1}$ activity would also reflect the endogenous expression of *Sox10* mRNA at later stages of NC-lineages. Combined with the Tol2-mediated gene transfer technique, embryos were electroporated with pT2K-enhancer$^{4\text{-}1}$-tkEGFP and pCAGGS-T2TP (Fig. 3A), and their DRGs were compared for EGFP signals and endogenous *Sox10* mRNA in alternate sections at different developmental stages. As the expression level of endogenous *Sox10* mRNA started to decrease at E4 onward (Fig. 3D), the number of EGFP$^+$ cells became smaller (Fig. 3B, views are obtained with the same exposure time; n = 6 for E3, E4, E5, and n = 3 for E6 and E7). Co-electroporated control vector, pT2K-CAGGS-mCherry, remained positive until E7 (Fig. 3C), indicating that the decline of EGFP signal was not due to a disappearance of the transgene. The decrease of EGFP signals was also quantitatively shown by the ratio of EGFP$^+$ cells over mCherry$^+$ cells in DRG (Fig. 3E). Together,

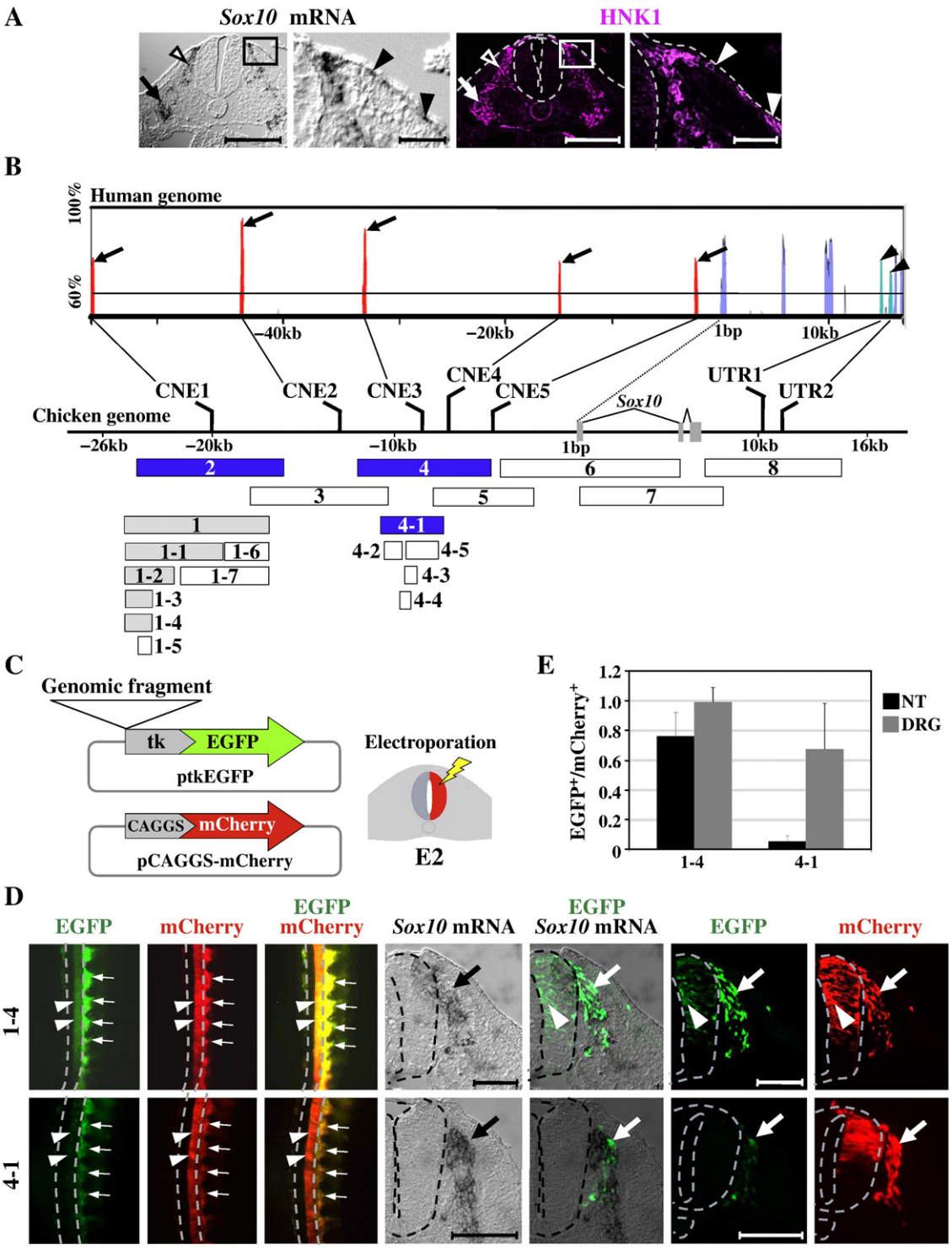

Fig. 2. Identification of NCC-specific enhancer of the *Sox10* gene. (A) Confirmation of NCC-specific expression of *Sox10* mRNA by in situ hybridization and HNK-1 immunohistochemical staining in neighboring histological sections. White arrowheads are developing DRGs, and arrows are sympathetic ganglia (scale bar: 100 μm). A square is enlarged where filled arrowheads indicated melanocyte precursors migrating underneath the epidermis (scale bar: 20 μm). (B) Comparison of genomic sequences using VISTA between human and chicken over 43 kb around the chicken *Sox10* gene. Conserved sequences where >60 bp homology over 100 bp are shown as sharp peaks. Five non-coding elements (CNE1–5, red peaks, arrows) were found in the 5′-region of *Sox10* ORF, and two UTRs (light blue peaks, arrowheads) in the 3′-region. Conserved sequences within the coding region are shown as light purple peaks. Eight larger genomic fragments (#1–#8), and 12 dissected fragments (#1-1–#1-7, #4-1–#4-5), were individually inserted into the reporter plasmid ptkEGFP (C), and assessed for their enhancer activity. Blue boxes are the fragments that showed a NCC-specific enhancer activity. Gray boxes were the fragments active both in the neural tube and NCCs. White boxes exhibited no enhancer activity (see also Table 2). (C) ptkEGFP inserted with a genomic fragment was co-electroporated into an E2 neural tube with pCAGGS-mCherry. (D) Enhancer activities of the fragments of #1-4 (neural tube and NCCs) and #4-1 (NCC). The left three photos are of the same dorsal views of E2.5 embryos. Arrowheads indicate the neural tube, $EGFP^{+}/mCherry^{+}$ with $enhancer^{1\text{-}4}$, $EGFP^{-}/mCherry^{+}$ with $enhancer^{4\text{-}1}$. Small arrows are segmentally formed DRGs, ($EGFP^{+}/mCherry^{+}$). Transverse views of these embryos are shown in the right 4 photos. Arrowheads are EGFP signal in the neural tube, and arrows indicate developing DRGs. Again, $enhancer^{4\text{-}1}$ is specifically active in DRG. Scale bars: 100 μm. (E) A ratio between $EGFP^{+}$ cells over $mCherry^{+}$ cells in the neural tube or DRG is shown. n = 12 for each.

Table 1
Description of CNEs. Positions in chicken genome, length (bp), and similarity between human and chicken sequences for each of CNEs (#1–#5) and UTRs (#1–#2) shown in Fig. 2.

Conserved noncoding element	Position in chicken sequence (bp)[a]	Length in chicken sequence	Similarity in human sequence
CNE1	−20,108 to −19,966	146 bp	72.60%
CNE2	−13,012 to −12,887	126 bp	94.40%
CNE3	−8526 to −8348	179 bp	85.50%
CNE4	−7078 to −6977	105 bp	71.40%
CNE5	−4658 to −4527	142 bp	69.50%
UTRl	10,124 to 10,243	120 bp	74.20%
UTR2	11,149 to 11,361	235 bp	68.10%

[a] The position of the *Sox10* translational initiation site is taken as +1 bp.

the activity of enhancer$^{4\text{-}1}$ identified in this study reflects the endogenous activity of the *Sox10* gene in both early and late DRGs.

Tol2-mediated gene transfer combined with Cre/loxP system using cultured cells

To overcome the inactivation of enhancer$^{4\text{-}1}$ in late NCC lineages, we combined the above mentioned expression methods with the Cre/loxP-mediated genetic recombination, the latter widely used in mouse genetics. The Cre/loxP system is useful to manipulate a specific cell lineage(s) because even a transiently active enhancer-Cre can lead to persistent expression of a gene (i.e. EGFP) if EGFP is manufactured to be driven by a constitutive promoter upon the Cre-mediated recombination (Gu et al., 1994; Hamilton and Abremski, 1984; Lobe et al., 1999; Nagy, 2000). We therefore combined the enhancer$^{4\text{-}1}$ and Cre/loxP system along with the Tol2-mediated genomic integration to achieve a persistent manipulation of late NCC lineages.

We first optimized the condition for such combined techniques using avian cell line DF1 (fibroblast) cultured in vitro. We prepared three kinds of plasmids (Fig. 4A): pCAGGS-T2TP, pxCANCre(pCAGGS-Cre), and pT2K-CAGGS-loxP-DsRed2-loxP-EGFP, which contains DsRed2-stop cassette and EGFP. Without Cre activity, DsRed2 is constitutively expressed by CAGGS promoter whereas Cre induces an excision of loxP-DsRed2-loxP (stop cassette), leading to constitutive EGFP expression driven by CAGGS (Fig. 4A).

We co-transfected these three plasmids into cultured DF1 cells. As expected, EGFP expression started by 3-day, and lasted until 25-day, when the assay was terminated (Fig. 3B, F). Two kinds of control experiments were performed, lacking either Cre (Fig. 3C) or transposase (Fig. 3D), respectively. Without Cre, although DsRed2 expression was stably retained, no EGFP-positive cells were observed (Fig. 3C). Without transposase, although the recombination occurred successfully displaying EGFP signals, such expression was transient (Fig. 3D). The data obtained by these control experiments indicate that the persistent EGFP expression seen in the culture with both transposase and Cre (Fig. 4B) was a result of genomic integration and Cre-mediated recombination occurring simultaneously in the cells.

The Cre-mediated recombination of genomically integrated plasmid in DF1 cells was also quantitatively assessed where the relative number of EGFP$^+$ cells was measured (EGFP$^+$ cells per 1000 cells). At 4-day post transfection, the index was similar between the culture transfected with the three plasmids (305 ± 14) and the control culture missing transposase (285 ± 21) (Fig. 4F). However, at 7-day onward, the index between these two cultures became different: 175 ± 33 with the three plasmids whereas 99 ± 3 for the control. By 15-day, although almost no EGFP$^+$ cells were found in the control, 98 ± 15 cells remained EGFP$^+$ in the culture with the three plasmids. In the other control that received no Cre (Fig. 4C), although Tol2-mediated genomic integration occurred successfully, they were all DsRed2$^+$ and no EGFP signal was found (Fig. 4C, F). Collectively, we conclude that the three plasmids used in this study enabled Cre-mediated recombination of Tol2-integrated exogenous genes, the first demonstration for avian cells.

We further examined whether the recombination of DsRed2-loxP stop cassette was dose-dependent of pxCANCre. Six different doses of pxCANCre plasmid were tested (Fig. 4E; 0.1 ng–50 ng). The number of EGFP$^+$ cells (recombined), DsRed2$^+$ cells (not recombined), and EGFP- and DsRed2-double positive cells were assessed per 300 transfected cells at 16-day post transfection. EGFP-positive cells were seen with 5 ng of pxCANCre, with the number becoming greater as the dose of pxCANCre increased (Fig. 4E). Accordingly, the ratio of DsRed2$^+$ cells decreased (Fig. 4G). Virtually no double-positive cells were observed. Thus, the recombination efficiency of DsRed2-loxP stop cassette depends on the dose of Cre protein.

NCC-specific and persistent expression of transgenes by combining Sox10-enhancer$^{4\text{-}1}$, Tol2-transposon, and Cre/loxP techniques

We further combined the Cre/loxP system with the NCC-specific enhancer to obtain persistent expression of transgenes in NCC-

Table 2
Details of the genomic fragments used for the enhancer activity assessments (see Fig. 2). Each fragment was inserted into the reporter plasmid ptkEGFP, followed by electroporation into early neural tube of chicken E2 embryos. NT: EGFP signals seen in neural tube/spinal cord. NCC: EGFP signal observed in early NCCs.

Genomic fragment	Position in chicken sequence (bp)[a]	Length in chicken sequence	Containing conserved noncoding element	Enhancer activity at E2.5 (st. 18)
1	−24,781 to −16,797	7985 bp	CNE1	NT, NCC
1–1	−24,781 to −19,255	5527 bp	CNE1	NT, NCC
1–2	−24,781 to −22,036	2746 bp		NT, NCC
1–3	−24,781 to −23,233	1549 bp		NT, NCC
1–4	−24,781 to −23,247	1535 bp		NT, NCC
1–5	−24,149 to −23,364	786 bp		None
1–6	−19,255 to −16,797	2459 bp		None
1–7	−21,736 to −16,797	4940 bp	CNE1	None
2	−24,161 to −15,997	8165 bp	CNE1	NCC
3	−17,947 to −10,223	7725 bp	CNE2	None
4	−11,994 to −4,645	7350 bp	CNE3, CNE4	NCC
4–1	−10,762 to −7,192	3571 bp	CNE3	NCC
4–2	−10,468 to −9426	1043 bp		None
4–3	−9554 to −8784	771 bp		None
4–4	−9767 to −9093	675 bp		None
4–5	−9237 to −7445	1793 bp	CNE3	None
5	−7829 to −2204	5626 bp	CNE4, CNE5	None
6	−4161 to 5771	9932 bp		None
7	157 to 8073	7917 bp		None
8	7097 to 14,637	7541 bp	UTR1, UTR2	None

[a] The position of the *Sox10* translational initiation site is taken as +1 bp.

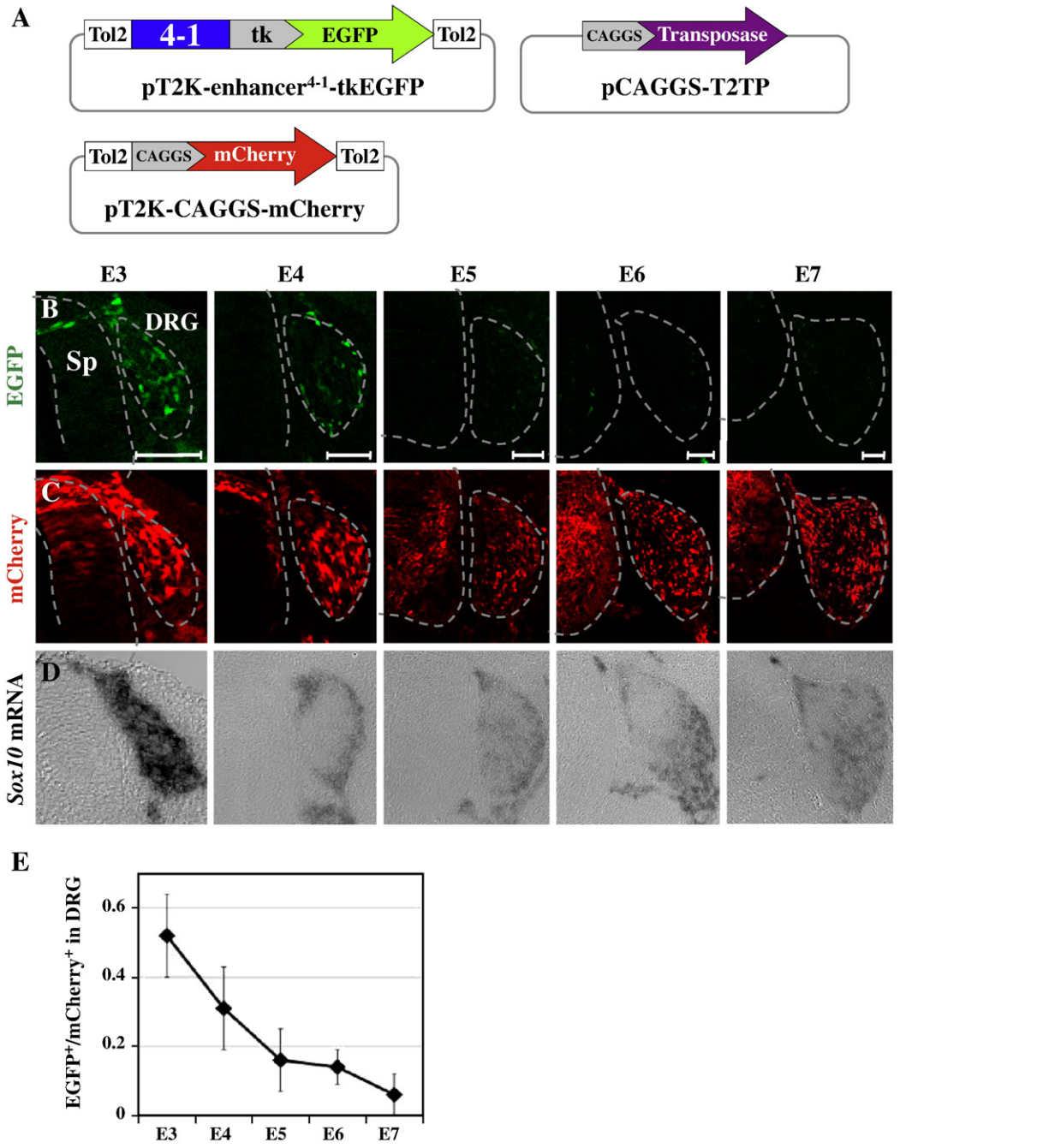

Fig. 3. Enhancer$^{4\text{-}1}$ activity reflects the expression of endogenous *Sox10* mRNA. The cassette of enhancer$^{4\text{-}1}$-tkEGFP was subcloned into the Tol2-vector (pT2K-enhancer$^{4\text{-}1}$-tkEGFP). The three plasmids shown in (A) were co-electroporated into the neural tube/NCCs. (B, C) Same views at each developmental stage. Although the stable integration was successful revealed by pT2K-CAGGS-mCherry, EGFP signal was diminished at E4 onward. (D) In situ hybridization of *Sox10* mRNA in neighboring sections of (B, C). Endogenous *Sox10* mRNA also diminished in DRG at E4 onward. Scale bars: 75 μm. (E) The decline of EGFP signal in DRG is quantitatively demonstrated. n = 10 for each developmental stage.

derived late lineages. The set of the plasmids was similar to Fig. 4, but pxCANCre was substituted for by pEnhancer$^{4\text{-}1}$-tk-Cre (Fig. 5A). The three plasmids were co-electroporated into early neural tube/neural crest at E2 as shown in Fig. 1, and EGFP signals in developing DRG were examined at E7. As expected, EGFP$^+$ cells were found specifically in DRG even though both DRG and spinal cord received transgenes (DsRed2$^+$) (Fig. 5A; n = 15). Two kinds of controls were carried out: one with pxCANCre (constitutive Cre activity), and the other with ptk-Cre (no Cre activity). When co-electroporated with pxCANCre, EGFP signals were found in both the spinal cord and DRG, showing that the excision of the DsRed2-stop cassette took place in all the electroporated cells (n = 10, Fig. 5B). When co-electroporated with ptk-Cre, virtually no EGFP$^+$ cells were observed although DsRed2$^+$ cells were widely distributed (n = 10, Fig. 5C), implying no recombination of the DsRed2-stop cassette. Together, these data indicate that the compound method using the three plasmids enables NCC-specific and persistent expression of transgenes that were stably integrated into chicken genome.

The NCC-specific and persistent expression was also observed in sensory neurons (Fig. 5D; n = 7), Schwann cells (Fig. 5E; n = 6), and melanocytes (Fig. 5F; n = 6) of E7 embryos in a flat-mounted surface tissue prepared as shown in Fig. 1.

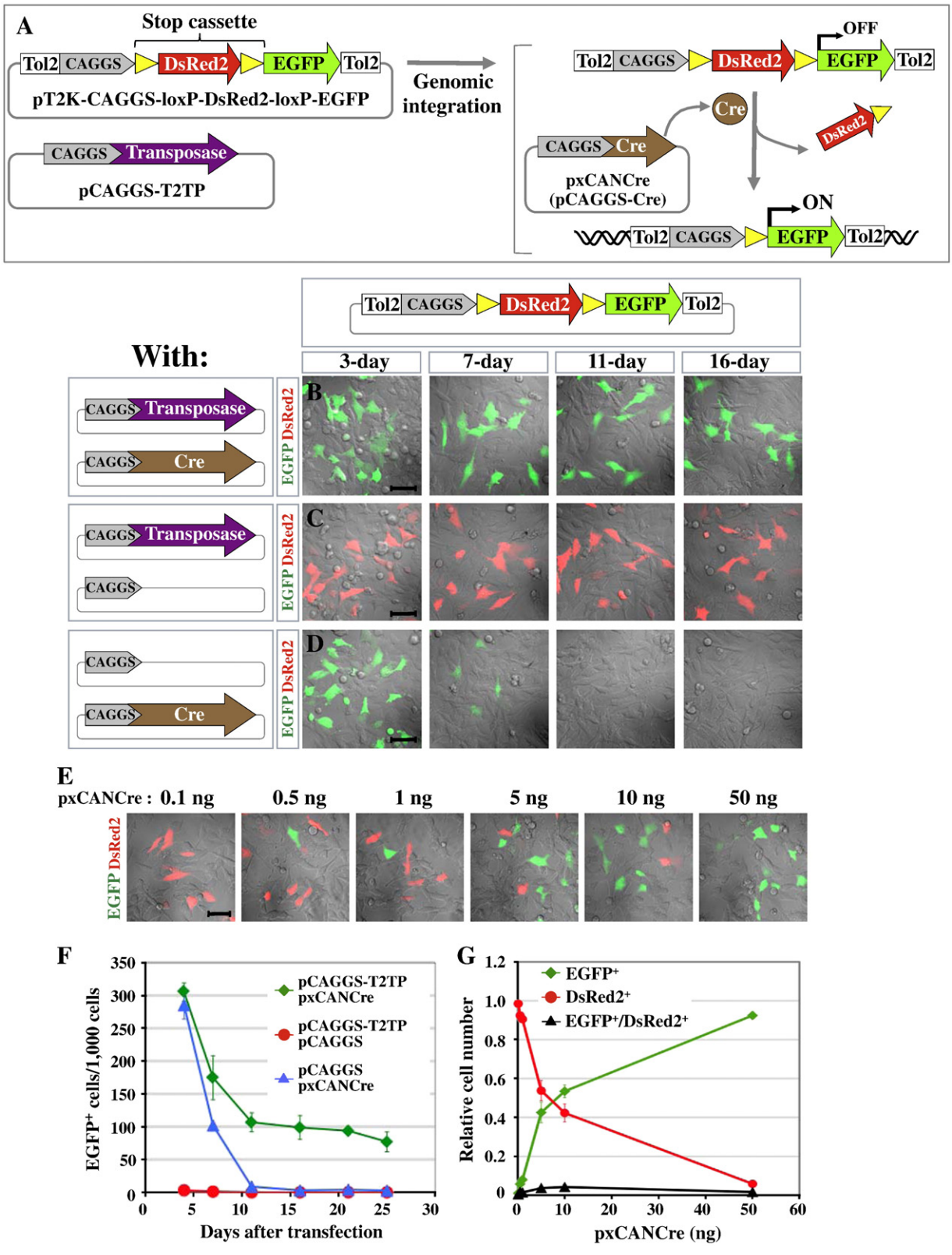

Fig. 4. Combination of Tol2-mediated genomic integration with Cre/loxP system assessed using cultured DF1 cells. (A) Schematic representation of the principle of the expression system. The stop cassette (DsRed2) is excised by Cre-activity, leading to constitutive expression of EGFP. (B–D) DF1 cells were co-transfected with pT2K-CAGGS-loxP-DsRed2-loxP-EGFP (shown on the top) and the plasmids indicated on the left. $EGFP^+$- and $DsRed2^+$ cells were assessed at different time points (n = 3 for each). (C, D) Control experiments. Scale bars: 50 μm. (E) DF1 cells were co-transfected with the same set of plasmids as in (B), with a range of doses of pxCANCre (pCAGGS-Cre), followed by the assessment after 16 days (n = 3 for each). (F) Quantitative representation of $EGFP^+$ cell or $DsRed2^+$ cells in the experiments shown in (B–D). (G) Quantitative representation of $EGFP^+$ cells, $DsRed2^+$ cells, or $EGFP^+/DsRed2^+$ cells in the experiments shown in (E).

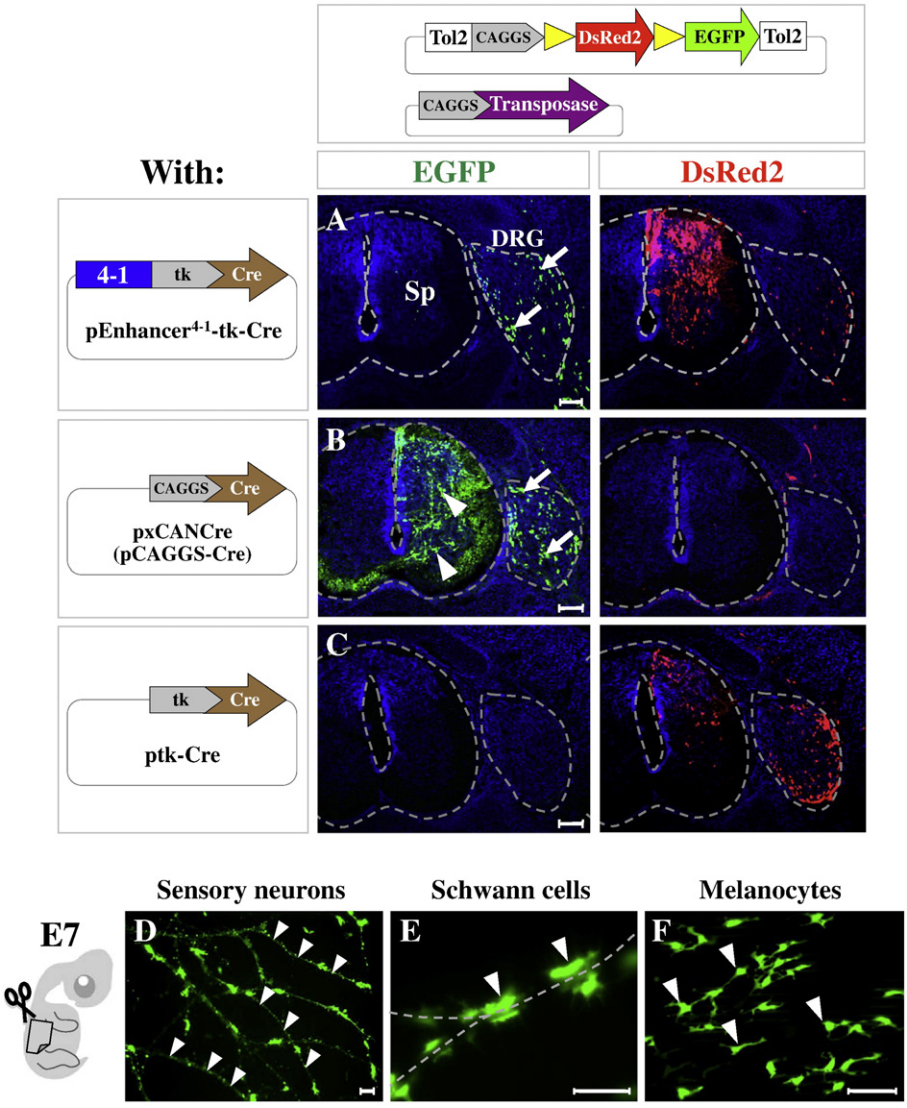

Fig. 5. NCC-specific and stable expression of electroporated genes in embryos by combining Tol2-Cre/loxP and *Sox10* enhancer$^{4\text{-}1}$. The design of experiments is similar to that shown in Fig. 4, with a substitution of *Sox10* enhancer$^{4\text{-}1}$-Cre for CAGGS-Cre, the latter used as a control in this experiment. (A–C) Plasmids were electroporated into a neural tube as shown in previous figures, followed by harvesting at E7. Compare a numerous number of EGFP^{+} cells found in DRG (A) to no EGFP^{+} cells in (C), showing successful Cre-mediated recombination. Note also no EGFP^{+} cells in the spinal cord (A), contrasting with (B), indicating a NCC-specific transgenesis. Remaining signal of DsRed2 in DRG (A, right) represents cells where Cre-mediated recombination failed to occur. Cre-activity by CAGGS was stronger than enhancer$^{4\text{-}1}$–Cre since DsRed2^{+} cells were not observed in (B). n = 15 for each. Scale bars: 100 μm. (D–F) Other types of NCC-derived cells also expressed EGFP stably at E7 of embryos treated as shown in (A); sensory neurons (D), Schwann cells (E), and melanocytes (F). Flat-mount specimens of surface tissues were prepared from E7 embryos as described in Fig. 1E–G. Scale bars: 50 μm.

Tetracycline-inducible expression of Cre/loxP-recombined genes

We previously optimized the method of tet-on expression of transgenes in chickens where electroporated genes can be activated in a temporally-regulated manner.

(Watanabe et al., 2007). This technique is also applicable to Tol2-mediated genomically integrated transgenes (Sato et al., 2007). We therefore extended our study to conditionally manipulate late-developing NCCs with transgenes in a spacio-temporally specific manner. Thus, we combined the tet-on expression method with the Tol2-integration and Cre/loxP techniques, referred to as Tol2-Cre/loxP-tet-on method.

Prior to embryonic application, we looked for the optimal condition using cultured DF1 cells. Four kinds of plasmids were used, two of which were as shown in Fig. 4 (pxCANCre and pCAGGS-T2TP). The EGFP-expression cassette is carried by pT2K-BI-TRE-EGFP (Watanabe et al., 2007). Briefly, EGFP is under the control of TRE (tetracycline responsive element), which is activated by rtTA2^{s}-M2 (reverse tet-controlled transcriptional activator) solely in the presence of doxycycline (Dox; analog of tetracycline). rtTA2^{s}-M2, subcloned into Tol2-loxP-DsRed2-containing vector to make pT2K-CAGGS-loxP-DsRed2-loxP-rtTA2^{s}-M2, (Fig. 6A), would be expressed upon the Cre-mediated excision of the stop cassette (loxP-DsRed2-loxP). Both the rtTA2^{s}-M2-containing cassette and EGFP-containing cassette were designed to be integrated into the genome (in pT2K-vector).

These four plasmids were co-transfected into DF1 cells, and they were cultured with or without Dox (Fig. 6B, C). Whereas a substantial number of cells expressed EGFP when added with Dox (Fig. 6B), EGFP was silent when added with PBS as a control (Fig. 6C). A similar experiment performed with Dox but lacking Cre yielded many DsRed2^{+} cells, but no EGFP^{+} cells (Fig. 6D). Thus, both Cre-mediated excision of the DsRed2 stop cassette and Dox-dependent activation by rtTA2^{s}-M2 took place simultaneously.

Similarly to Fig. 4F, EGFP expression was persistently retained at least until 21-day after transfection (Fig. 6E), confirming the Tol2-mediated genomic integration. However, the relative number of EGFP^{+}

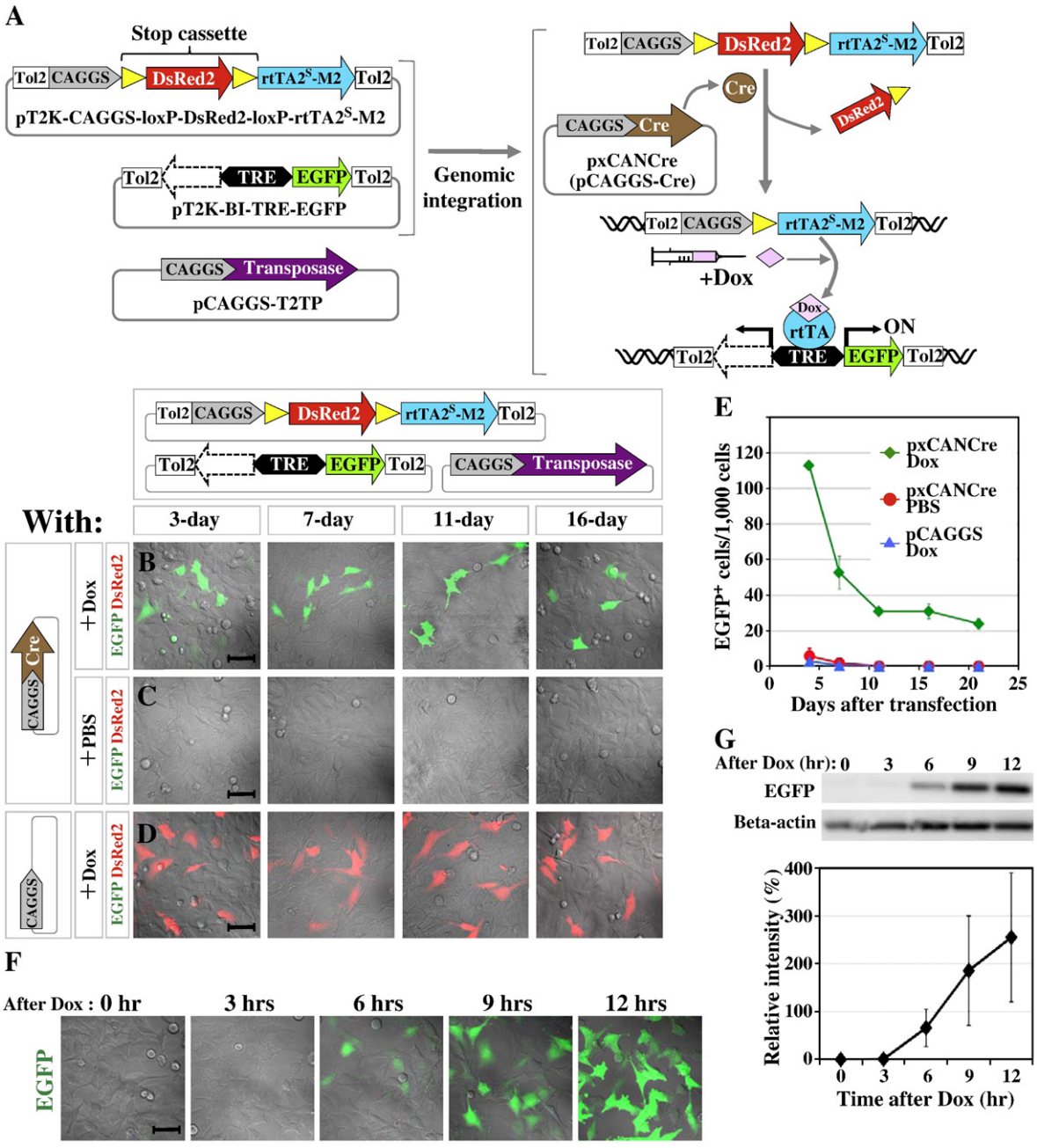

Fig. 6. Tet-on inducible expression combined with Tol2-Cre/loxP system assessed with cultured DF1 cells. This is to add an inducible expression system to the previous expression method established in Fig. 4. (A) Here, the Cre-mediated recombination leads to the expression of rtTA2^S-M2 instead of EGFP. In the presence of Dox, this transactivator is bound to TRE, activating expression of EGFP that is carried by pT2K-BI-TRE-EGFP. Since both the rtTA2^S-M2-containing cassette and TRE-EGFP-containing cassette are genomically integrated by Tol2, the tet-on manipulation (by injecting Dox solution) is available at late stages of development. (B–D) DF1 cells were co-transfected with three plasmids (top) and those shown on the left, and assessed for EGFP- and DsRed2 signals at different time points. (C, D) Control experiments. In the presence of Cre and Dox, EGFP was induced to be expressed. Scale bars: 50 μm. (E) Quantitative representation of EGFP$^+$ cells in the experiments shown in (B–D). (F) Time-course of Dox-induced expression of EGFP. After transfection with the same set of plasmids shown in (B), three cell lines were established, which expressed EGFP in a Dox-dependent manner. After adding with Dox (0 h), EGFP-positive cells were counted at different time points. EGFP signal increased at 6 h onward. (G) The increase in EGFP signal observed in (F) was also confirmed by Western blot analyses, with a quantitative representation.

cells at 21-day was ~2.4%, and this is smaller than ~10% observed in Fig. 4F. In the expression system shown in Fig. 6, two different plasmids need to be simultaneously integrated into the genome of the same cell, the incidence occurring at a lower efficiency than a single integration.

We further analyzed a time course of EGFP expression during Dox-induction. After transfection with the 4 plasmids as shown above, we obtained three stable DF1 cell lines that expressed EGFP in a Dox-dependent manner. At 6-h post Dox, cells started to express EGFP, and the number of EGFP$^+$ cells became greater onward (Fig. 6F). The increase in EGFP-signal was also confirmed by Western blot analyses (Fig. 6G). These data show that Dox needs to be administered at least 6 h prior to the TRE-driven activation of genes.

TRE is a bidirectional promoter, which can simultaneously activate two genes subcloned in opposite directions. Although we solely used EGFP in this study with the other direction being vacant, any gene to be tested can be conditionally expressed by Dox administration together with EGFP.

Tet-on inducible expression of stable transgenes in a NCC-specific manner

Finally, the methods developed above were applied to conditionally manipulate late-developing NCC lineages with transgenes in a spacio-temporally controlled manner. For embryonic NCC manipulation, a similar set of the 4 plasmids was used, but this time Cre expression was driven by *Sox10* enhancer (pEnhancer$^{4\text{-}1}$-tk-Cre) instead of CAGGS (Fig. 7A). These plasmids were co-electroporated into neural tube/neural crest at E2, followed by Dox injection at E5. Before the Dox injection, no EGFP^{+} cells were found in the spinal cord or DRG, whereas DsRed2 signal was widely distributed in these tissues (Fig. 7B, n = 16). Following Dox injection, EGFP signals were seen in DRG at E6 (n = 11) and E7 (n = 14). Importantly, they were not found in the spinal cord (Fig. 7C, D). DsRed2^{+} cells were occasionally seen in DRG, with the cell number varying between specimens (Fig. 7C, D). This was probably the case where enhancer$^{4\text{-}1}$-Cre activity was insufficient to excise the DsRed2 stop cassette. In control embryos

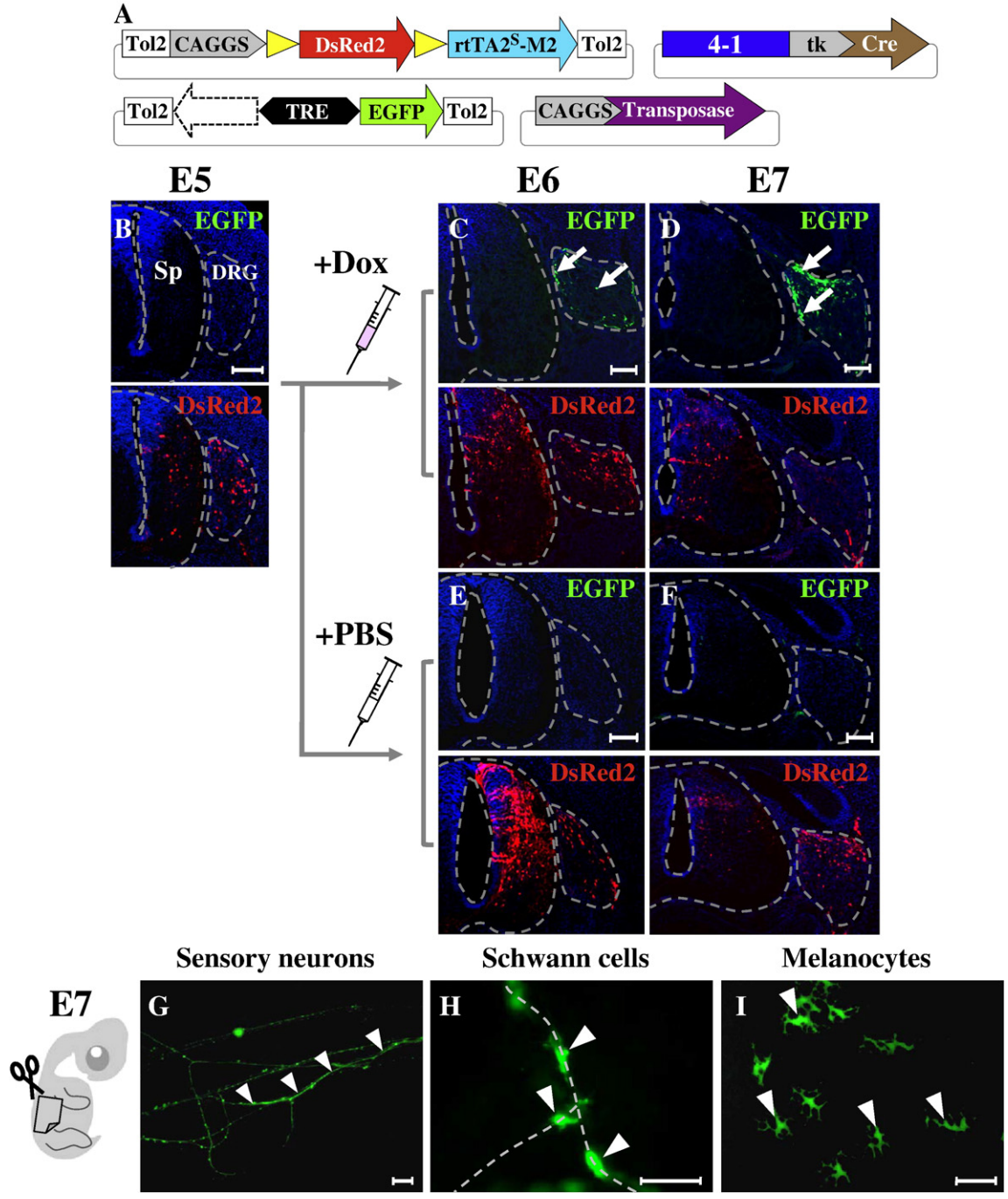

Fig. 7. Combination of tet-on system with Tol2-Cre/loxP and *Sox10* enhancer$^{4\text{-}1}$. (A) The design of experiments is similar to that shown in Fig. 6, with a substitution of *Sox10* enhancer$^{4\text{-}1}$-Cre for CAGGS-Cre (Fig. 6). (B–F) The four plasmids were electroporated into a neural tube as shown in previous figures, followed by assessment at E6 and E7. Prior to Dox injection, no EGFP-positive cells were found in DRG whereas DsRed2-positive cells were seen both in the spinal cord and DRG (B). In contrast, successful induction of EGFP signal was observed after Dox (C, D). No EGFP-positive cells were detected in embryos injected with PBS (E, F). Scale bars: 100 μm. (G–I) In E7 embryos as shown in (D), other types of NCC-derived cells were also Dox-induced to express EGFP; sensory neurons (G), Schwann cells (H), and melanocytes (I). Flat-mount specimens of surface tissues were prepared from E7 embryos as described in Figs. 1E–G, and 5D–F. n = 10 for each. Scale bars: 50 μm.

injected with PBS, no EGFP$^+$ cells were found whereas DsRed2 signal was persistent in both DRG and spinal cord at E6 (n = 15, Fig. 7E) and E7 (n = 12, Fig. 7F). Thus, the compound expression system, Tol2-enhancer$^{4\text{-}1}$-Cre/loxP-tet-on, permits a temporally inducible manipulation with transgenes in NCC-specific lineages of late developing embryos. This was also evident in sensory neurons, Schwann cells, and melanocytes in E7 embryos (Fig. 7G–I, n = 3 for each), observed in a flat-mount specimen.

The compound methods allowed ex vivo direct visualization of individual Schwann cells associated with peripheral axon bundles

To prove that the methods described above were indeed powerful to gain mechanistic insights into late development of NCCs in vivo, we focused on cellular activity of Schwann cells associated with axons in peripheral tissues. In particular, we exploited the advantage of the methods permitting analyses at a single cell resolution in three-dimensional environment/in vivo. For this purpose, we used the method described in Fig. 5, the combination of *Sox10*-enhancer$^{4\text{-}1}$, Tol2-transposon, and Cre/loxP. In the course of aforementioned experiments, we had noticed that the activity of *Sox10*-enhancer$^{4\text{-}1}$ was not sufficient to achieve a complete excision of loxP-DsRed2-loxP (stop cassette), thus leading to mosaic labeling of NCC-derived cells with EGFP (recombined by Cre) or DsRed2 (not recombined by Cre) (Fig. 5A, Fig. 7C, D). We therefore exploited such idleness of enhancer$^{4\text{-}1}$ to obtain Schwann cells and peripheral axons that were simultaneously labeled with different fluorescents; stochastically, a EGFP-labeled Schwann cell was found near DsRed2-positive axon(s), or vice versa. Electroporated embryos were cut into slices, and a slice that contained differently colored Schwann cell(s) and axon(s) was subjected to confocal time-lapse microscopy. We paid attention to sensory neurons, which were efficiently and reproducibly labeled with either DsRed2 or EGFP (see above).

At E3.5, when a majority of Schwann cells were found near extending axon bundles, these cells were amorphic, and exhibited active cellular processes, including lamellipodia and filopodia, that repeatedly extended and retracted. These processes were randomly directed (n = 5, Fig. 8A, Movie 1). At E4.5, the behavior of labeled Schwann cells was largely similar to that seen at E3.5. Several cells were prone to be closely attached to axons. Occasionally, cellular processes were seen traversing several axons (n = 7, Fig. 8B, Movie 2). At E7, in clear contrast, Schwann cells were profoundly elongated with a thin cell body with a tight association with axons bundles. These cells were static with little cellular processes (n = 6, Fig. 8C, Movie 3).

Until present, all the studies reporting behaviors of Schwann cells along axons were performed in vitro using cultured cells, where

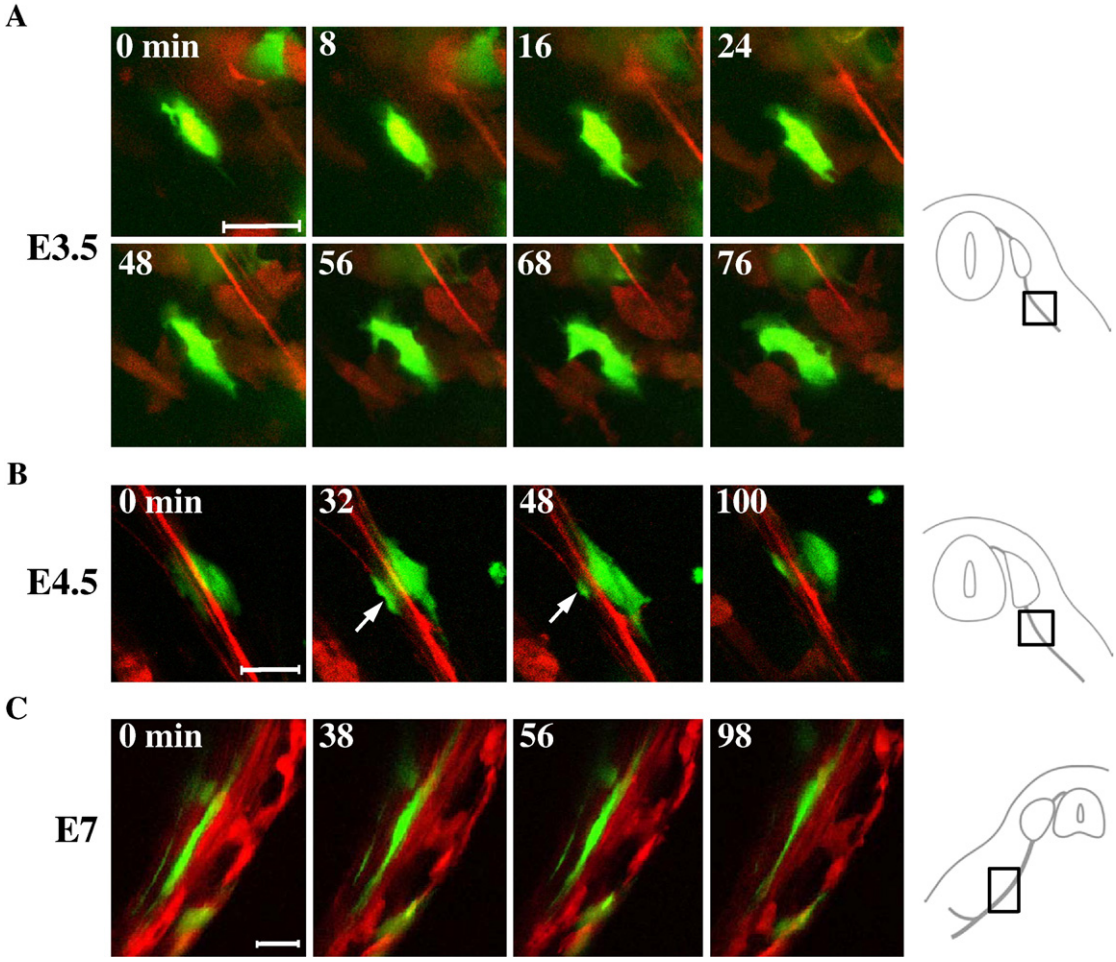

Fig. 8. Time-lapse live-imaging confocal microscopy to simultaneously visualize EGFP-labeled Schwann cell(s) and DsRed2-labeled sensory axons in the same view. Three different developmental stages were shown (A) E3.5, (B) E4.5, and (C) E7. In all specimens, ex vivo cultured slices were prepared from embryos into which pCAGGS-T2TP, pEnhancer$^{4\text{-}1}$-tk-Cre, and pT2K-CAGGS-loxP-DsRed2-loxP-EGFP were co-electroporated. Views containing EGFP-positive Schwann cell(s) associated with DsRed2-positive axon(s) of sensory neurons were live-imaged using a 40× Plan-Apochromat objective lens. The photos are part of the movies 1–3 (Supplementary materials). (A) E3.5 Schwann cells exhibited active extension and retraction of lamellipodia and filopodia-like processes, which were protruded to random direction. (B) E4.5 EGFP-positive Schwann cells often showed filopodia-like structures parallel to the axons, and occasionally extended a process traversing several axons (arrows). (C) E7 EGFP-positive Schwann cells were closely associated with DsRed2-positive sensory neurons. The cells were profoundly elongated and static with little cellular processes. Location and orientation of the recorded specimens are as shown in a diagram (right). Scale bars: 20 μm.

Schwann cells were sparsely distributed on axons, the condition significantly different from in vivo (Yu et al., 2009).

In those studies, although some filopodia-like protrusions by naïve Schwann cells were observed, the cease of such activities and the time course of cell elongation were unattended. It is conceivable by our findings that in normal environment, naïve Schwann cells actively show cellular protrusions as amorphic cells, and as the cells become mature, they increasingly fill the surface of nearby axons with a tight association between them, resulting in the cease of protrusion of cellular processes. Further studies are awaited to unveil how these changes in cell behavior are regulated. Together, the ex vivo visualization of Schwann cells at a single cell level, allowed for the first time by virtue of the method described in this study, provides new insights into the association of developing Schwann cells with nearby axons in vivo. Our findings also underscore the importance of NCC studies of in the actual body.

Conclusion

In this study we have developed compound methods with which transgenes are persistently or conditionally manipulated in NCC-derived lineages of late developing embryos (Fig. 9). The usefulness of these methods has subsequently been proved by a direct and simultaneous visualization of EGFP-labeled Schwann cells and DsRed2-labeled axons in three dimensional environment. This unprecedented approach has provided novel aspects of cellular behavior and activities of Schwann cells when they are associated with axon bundle structures in peripheral tissues.

Four types of compound methods have been developed. First, the Tol2-mediated genomic integration method has enabled persistent expression of electroporated genes in cells including NCC-derived lineages (Fig. 9A). This persistent expression is particularly valuable because unlike central nervous system the NCCs are highly proliferative and therefore non-integrated genes disappear rapidly. Second, a combination of the Tol2-method with the NCC-enhancer (enhancer$^{4\text{-}1}$), identified in this study, drives NCC-specific expression of transgenes. This is useful particularly when sensory neurons or Schwann cells (NCC-derived) need to be manipulated separately from closely related tissues, i.e. motor neurons (Fig. 9B). Third, Cre/loxP-mediated DNA recombination further adds advantages that NCC-derived cells are specifically and persistently manipulated regardless of a declined activity of *Sox10* enhancer at later stages (Fig. 9C). Fourth, we have further combined these methods with the tet-on expression technique by which expression of transgenes can be induced at a desired time point during NCC differentiation (Fig. 9D). This permits conditional manipulation of late-developing NCC lineages with exogenous genes. Last, by exploiting these methods, we have, for the first time, succeeded in direct visualization of axon-associated Schwann cells at a single cell level in vivo/ex vivo. They show previously unappreciated behaviors, which depend on developmental stages. Our

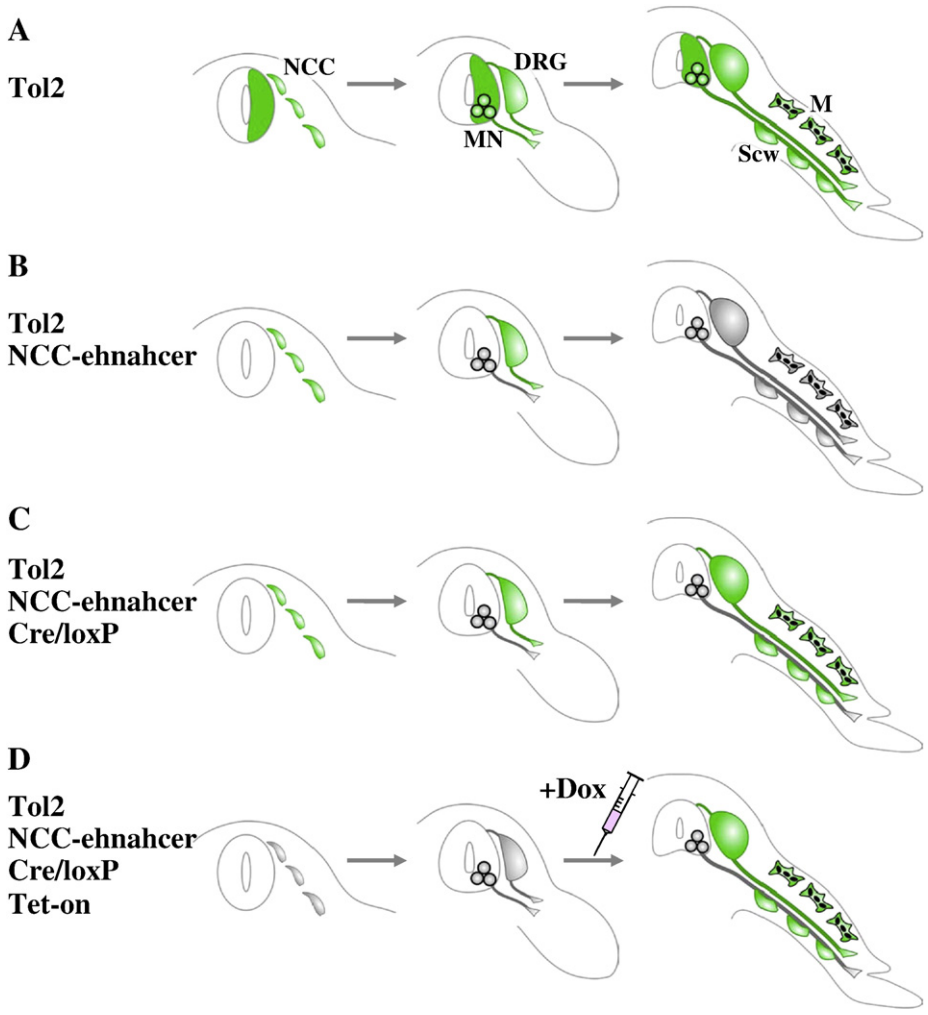

Fig. 9. Schematic demonstration of the summary of this study. Early, middle, and late stages of electroporated embryos are represented, where early NCCs and late developing NCC-derivatives are shown. Motor neurons, non-NCC-origin, are also EGFP-labeled unless NCC-enhancer is used (A). Increasingly compound methods (from A to D) permit non-specific but stable (A), NCC-specific but not persistent (B), NCC-specific and persistent (C), and NCC-specific, persistent, and temporally controlled manipulations (D) with exogenous genes. See text for detailed explanation. MN: motor neurons, M: melanocytes, Scw: Schwann cells.

study has opened a novel way to investigate at molecular and cellular levels how the late NCC development is regulated, the long-standing but yet unsolved question. The principles described in this study will also be applicable to other embryonic cell lineages where tissue-specific enhancers are available.

Supplementary materials related to this article can be found online at doi:10.1016/j.ydbio.2011.02.001.

Acknowledgments

We are grateful to Dr. H. Kondoh (Osaka University) for ptkEGFP and valuable advices. We thank Dr. I. Saito (University of Tokyo) for pxCANCre and pCALNL5, and Dr. K. Emoto (Osaka Bioscience Institute), Dr. S. Nakagawa (RIKEN) and Y. Atsuta (NAIST) for helpful discussion. This work was supported by a Grant-in-Aid for Scientific Research on Innovative Areas, and Grant-in-Aid for Scientific Research (A) from the Ministry of Education, Culture, Sports, Science and Technology of Japan, the Global COE program (Frontier Biosciences: Strategies for Survival and Adaptation in a Changing Global Environment), MEXT, Japan, and CREST (JST).

References

Betancur, P., Bronner-Fraser, M., Sauka-Spengler, T., 2010. Genomic code for Sox10 activation reveals a key regulatory enhancer for cranial neural crest. Proc. Natl Acad. Sci. USA 107, 3570–3575.

Betters, E., Liu, Y., Kjaeldgaard, A., Sundstrom, E., Garcia-Castro, M.I., 2010. Analysis of early human neural crest development. Dev. Biol. 344, 578–592.

Cheng, Y., Cheung, M., Abu-Elmagd, M.M., Orme, A., Scotting, P.J., 2000. Chick sox10, a transcription factor expressed in both early neural crest cells and central nervous system. Brain Res. Dev. Brain Res. 121, 233–241.

Funahashi, J., Okafuji, T., Ohuchi, H., Noji, S., Tanaka, H., Nakamura, H., 1999. Role of Pax-5 in the regulation of a mid-hindbrain organizer's activity. Dev. Growth Differ. 41, 59–72.

Gu, H., Marth, J.D., Orban, P.C., Mossmann, H., Rajewsky, K., 1994. Deletion of a DNA polymerase beta gene segment in T cells using cell type-specific gene targeting. Science 265, 103–106.

Hamilton, D.L., Abremski, K., 1984. Site-specific recombination by the bacteriophage P1 lox-Cre system. Cre-mediated synapsis of two lox sites. J. Mol. Biol. 178, 481–486.

Harris, M.L., Hall, R., Erickson, C.A., 2008. Directing pathfinding along the dorsolateral path - the role of EDNRB2 and EphB2 in overcoming inhibition. Development 135, 4113–4122.

Himly, M., Foster, D.N., Bottoli, I., Iacovoni, J.S., Vogt, P.K., 1998. The DF-1 chicken fibroblast cell line: transformation induced by diverse oncogenes and cell death resulting from infection by avian leukosis viruses. Virology 248, 295–304.

Kanegae, Y., Takamori, K., Sato, Y., Lee, G., Nakai, M., Saito, I., 1996. Efficient gene activation system on mammalian cell chromosomes using recombinant adenovirus producing Cre recombinase. Gene 181, 207–212.

Knecht, A.K., Bronner-Fraser, M., 2002. Induction of the neural crest: a multigene process. Nat. Rev. Genet. 3, 453–461.

Le Douarin, N.M., Kalcheim, C., 1999. The Neural Crest2nd Edition. Cambridge University Press.

Lobe, C.G., Koop, K.E., Kreppner, W., Lomeli, H., Gertsenstein, M., Nagy, A., 1999. Z/AP, a double reporter for cre-mediated recombination. Dev. Biol. 208, 281–292.

Mayor, C., Brudno, M., Schwartz, J.R., Poliakov, A., Rubin, E.M., Frazer, K.A., Pachter, L.S., Dubchak, I., 2000. VISTA : visualizing global DNA sequence alignments of arbitrary length. Bioinformatics 16, 1046–1047.

McKeown, S.J., Lee, V.M., Bronner-Fraser, M., Newgreen, D.F., Farlie, P.G., 2005. Sox10 overexpression induces neural crest-like cells from all dorsoventral levels of the neural tube but inhibits differentiation. Dev. Dyn. 233, 430–444.

Meulemans, D., Bronner-Fraser, M., 2004. Gene-regulatory interactions in neural crest evolution and development. Dev. Cell 7, 291–299.

Momose, T., Tonegawa, A., Takeuchi, J., Ogawa, H., Umesono, K., Yasuda, K., 1999. Efficient targeting of gene expression in chick embryos by microelectroporation. Dev. Growth Differ. 41, 335–344.

Nagy, A., 2000. Cre recombinase: the universal reagent for genome tailoring. Genesis 26, 99–109.

Ohata, E., Tadokoro, R., Sato, Y., Saito, D., Takahashi, Y., 2009. Notch signal is sufficient to direct an endothelial conversion from non-endothelial somitic cells conveyed to the aortic region by CXCR4. Dev. Biol. 335, 33–42.

Petiot, A., Ferretti, P., Copp, A.J., Chan, C.T., 2002. Induction of chondrogenesis in neural crest cells by mutant fibroblast growth factor receptors. Dev. Dyn. 224, 210–221.

Sato, Y., Yasuda, K., Takahashi, Y., 2002. Morphological boundary forms by a novel inductive event mediated by Lunatic fringe and Notch during somitic segmentation. Development 129, 3633–3644.

Sato, Y., Kasai, T., Nakagawa, S., Tanabe, K., Watanabe, T., Kawakami, K., Takahashi, Y., 2007. Stable integration and conditional expression of electroporated transgenes in chicken embryos. Dev. Biol. 305, 616–624.

Southard-Smith, E.M., Kos, L., Pavan, W.J., 1998. Sox10 mutation disrupts neural crest development in Dom Hirschsprung mouse model. Nat. Genet. 18, 60–64.

Tucker, R.P., 2001. Abnormal neural crest cell migration after the in vivo knockdown of tenascin-C expression with morpholino antisense oligonucleotides. Dev. Dyn. 222, 115–119.

Uchikawa, M., Ishida, Y., Takemoto, T., Kamachi, Y., Kondoh, H., 2003. Functional analysis of chicken Sox2 enhancers highlights an array of diverse regulatory elements that are conserved in mammals. Dev. Cell 4, 509–519.

Urlinger, S., Baron, U., Thellmann, M., Hasan, M.T., Bujard, H., Hillen, W., 2000. Exploring the sequence space for tetracycline-dependent transcriptional activators: novel mutations yield expanded range and sensitivity. Proc. Natl Acad. Sci. USA 97, 7963–7968.

Watanabe, T., Saito, D., Tanabe, K., Suetsugu, R., Nakaya, Y., Nakagawa, S., Takahashi, Y., 2007. Tet-on inducible system combined with in ovo electroporation dissects multiple roles of genes in somitogenesis of chicken embryos. Dev. Biol. 305, 625–636.

Yu, W.M., Chen, Z.L., North, A.J., Strickland, S., 2009. Laminin is required for Schwann cell morphogenesis. J. Cell Sci. 122, 929–936.